AUTHOR(S):

Huo, Wenting; Miki, Koji; Tokunaga, Daisuke; Mu, Huiying; Oe, Masahiro; Harada, Hiroshi; Ohe, Kouichi

Dual-Stimuli-Responsive Probes for Detection of Ovarian Cancer Cells and Quantification of Both pH and Enzyme Activity

Wenting Huo,[1] Koji Miki,*[1] Daisuke Tokunaga,[1] Huiying Mu,[1] Masahiro Oe,[1] Hiroshi Harada,[2] and Kouichi Ohe*[1]

[1]Department of Energy and Hydrocarbon Chemistry, Graduate School of Engineering, Kyoto University, Nishikyo-ku, Kyoto 615-8510

[2]Laboratory of Cancer Cell Biology, Graduate School of Biostudies, Kyoto University, Yoshida, Sakyo-ku, Kyoto 606-8501

E-mail: kojimiki@scl.kyoto-u.ac.jp (K. Miki), ohe@scl.kyoto-u.ac.jp (K. Ohe)
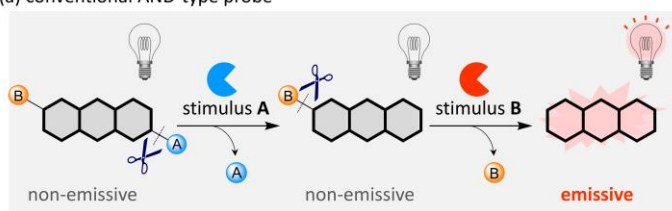
Abstract

Many physiological processes involve multiple coordinated chemical and/or biological events. Therefore, it is considered urgent to develop dual-responsive probes for a more comprehensive understanding of the synergistic effects between multiple analytes in complex cellular environments. In this study, we developed a dual-responsive probe **βgal-BP-PMB** (β-galactosyl–3,3′-dihydroxy-2,2′-bipyridyl–*p*-methoxybenzyl), the photoluminescence of which can be activated by β-galactosidase (β-gal) and acidic conditions. The overexpression of β-gal is an important feature of senescent and ovarian cancer cells. Single-input activatable probes for detecting β-gal activity in ovarian cancer cells can induce a false positive response from senescent cells. Because the lysosomal pH in senescent cells is increased, probe **βgal-BP-PMB** can be specifically activated in ovarian cancer cells, but silenced in senescent cells. Probe **βgal-BP-PMB** has a small molecular size, high sensitivity towards targeted stimuli and unique ratiometric properties, thereby enabling the quantification of both pH and enzyme activity. Such dual-responsive probes could earn a unique place in the field of bioimaging, where multiple analytes should be accurately and simultaneously monitored.

1. Introduction

Normal physiological processes are maintained through the precise control of biological and chemical compositions such as pH, ion concentrations and enzyme expression levels. Abnormal changes in these compositions are associated with a number of malignant diseases. Over the past few decades, numerous single-input activatable photoluminescent probes have been reported as indicators to measure changes in intracellular environments because they offer high sensitivity, non-invasiveness, and fast response.[1–7] However, the features of some natural processes are similar to those of targeted diseases. For example, β-galactosidase (β-gal), a lysosomal enzyme that catalyzes the cleavage of a β-galactosyl moiety, is known to be overexpressed in ovarian cancer cells.[8–13] The overexpression of β-gal is also observed in senescent cells (physiologically normal for humans at any age).[14] In this case, single-input β-gal responsive photoluminescent probes for detecting ovarian cancer cells can induce a false positive response from senescent cells. Normally, β-gal shows maximal activity between pH 4.0 and pH 4.5 in the lysosomes of ovarian cancer cells, but remarkably lower activity at pH 6.0. In senescent cells, β-gal maintains a detectable activity in lysosomes, pH 6.0.[15] Therefore, it is considered urgent to develop dual-responsive probes whose activations require both β-gal and pH 4.5 conditions to achieve a more specific detection of ovarian cancer cells.[16]

(a) conventional AND-type probe

non-emissive → stimulus A → non-emissive → stimulus B → emissive

(b) this work

βgal-BP-PMB
non-emissive
→ β-gal →
BP-PMB
emissive (450 nm)
→ pH~4.5 →
BP
emissive (480 nm)

✔ small luminophore ✔ large Stokes shift ✔ no false response ✔ quantification
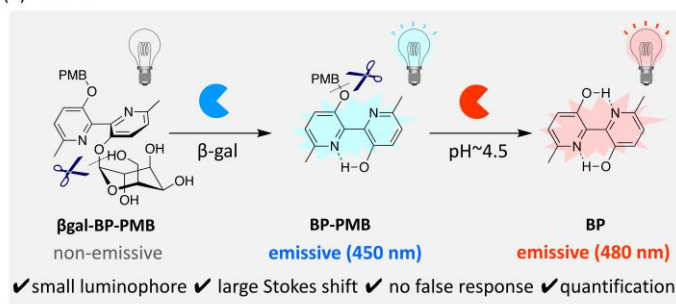
Figure 1. (a) Diagram of conventional AND-type dual-responsive photoluminescent probes. (b) Stepwise dual-responsive photoluminescent probes (this work).

Several 'AND-type' probes that can respond to two concurrently generated biological stimuli, especially to an enzyme, have been reported (Figure 1a). The reported dual-responsive 'AND-type' luminescent probes can be divided into two classes: (1) small luminophores with a small Stokes shift[17–20] and (2) multiple dye conjugates utilizing Förster resonance energy transfer (FRET).[21–23] In the former case, the large overlapping area between excitation and emission bands sometimes leads to poor detection sensitivity.[24] In the latter case, the large molecular size and structural complexity of FRET-based dyes may alter the intracellular environments and enzyme activity.[25–28] Furthermore, 'AND-type' probes cannot simultaneously quantify two stimuli, such as enzyme activity and ion concentration, by simply measuring the photoluminescent output. Hence, there is a strong requirement for the development of small dual-responsive probes with a large Stokes shift that can be applied to the ratiomeric quantification of enzyme activity.

3,3′-Dihydroxy-2,2′-bipyridyl **BP**[29-31] (molecular weight ≤220) is considered one of the smallest luminophores. Because the excited energy is relaxed through tautomerization related to hydrogen bonds—so-called excited-state intramolecular double proton transfer (ESIDPT)[32-35]—strong photoluminescence (PL) with a large Stokes shift is observed in aqueous solutions of **BP**.[29,30] Although its attractive PL properties are considered suitable in terms of dual-responsive probes, the application of **BP** as a sensor for enzyme activity has not yet been explored. Hence, in this study, we have created unsymmetrically functionalized **BP** with different substituents on its hydroxy groups to develop the dual-responsive probe **βgal-BP-PMB** (β-galactosyl–3,3′-dihydroxy-2,2′-bipyridyl–p-methoxybenzyl), which can respond to β-gal and acidic conditions in a stepwise fashion to form planar emissive **BP** (Figure 1b). Due to the different emission bands between **BP** and the intermediary monosubstituted **BP** derivative, unsymmetric **BP** derivatives, as probes, enable the quantification of both pH and enzyme activity, to which the reported 'AND-type' dual-responsive probes[18–20] are inaccessible (Figure 1a). Furthermore, we successfully applied **βgal-BP-PMB** to the recognition of β-gal-overexpressed ovarian

cancer cells without detecting a false positive response from senescent cells.

2. Results and Discussion

Design and synthesis. The unsymmetric structure of **BP** derivatives is essential for realizing its dual-responsive function. However, to date, a practical synthetic method for such unsymmetric or monoprotected **BP** derivatives has not been reported.[36] Straightforward synthesis through the acetylation or etherification of **BP** is unsuccessful because the hydroxy group of monoprotected **BP** is more reactive than that of **BP** owing to the disruption of hydrogen bonds (Fugure 2). Among the transformations examined, the Pd- and Cu-catalysed Stille coupling reaction efficiently afforded the unsymmetric **BP** derivative **Ac-BP-PMB**, having an acetyl (Ac) group and a *p*-methoxybenzyl (PMB) group, in good yield. The base-mediated deprotection of an Ac group quantitatively afforded monoprotected **BP-PMB**. Because an Ac group of **Ac-BP-PMB** can be readily replaced by other functional groups that specifically respond to the biomarkers of tumour cells, we next synthesized the acid- and β-gal-responsive probe **βgal-BP-PMB** via the classic Koenigs–Knorr glycosidation reaction[37] of **BP-PMB** (Figure 2). The UV-vis absorbance and photoluminescence spectra of bipyridyls were measured (Figure S1) and their photophysical properties were summarized in Table 1. The double-protected **βgal-BP-PMB** shows almost no PL emission and extremely low quantum yield. On the contrary, the
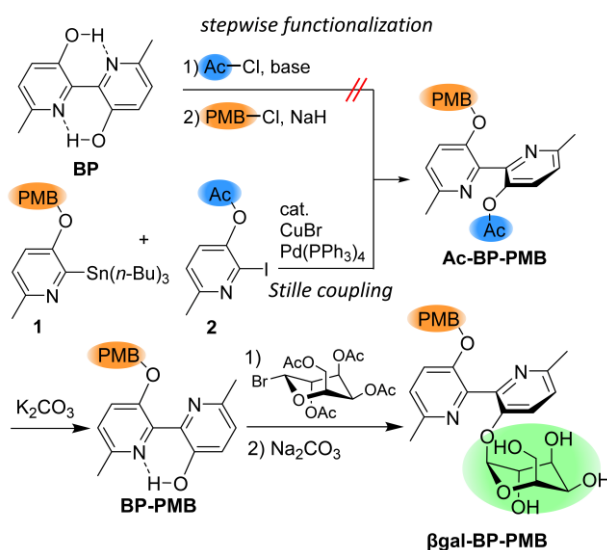
京都大学
KYOTO UNIVERSITY

A Self-archived copy in
Kyoto University Research Information Repository
https://repository.kulib.kyoto-u.ac.jp

京都大学学術情報リポジトリ
KURENAI 紅
Kyoto University Research Information Repository

Figure 2. Synthesis of unsymmetric bipyridyl **Ac-BP-PMB** and **βgal-BP-PMB**, and mono-protected **BP-PMB.**

Table 1. Photophysical properties of bipyridyls.[a]

compound	absorbance		fluorescence	
	λ_{max} (nm)	ε ($cm^{-1}M^{-1}$)	λ_{max} (nm)	Φ_{ref}
BP	355	6.6×10^3	479	0.057
	418	2.1×10^3		
BP-PMB	297	8.6×10^3	450	0.072
βgal-BP	293	1.0×10^3	438	0.0397
	340	2.2×10^3		
βgal-BP-PMB	292	7.3×10^3	–	<0.001

[a]In H_2O.

[b]λ_{ex} = 350 nm. Reference compound: Hoechst 33342 (= 0.034 in H_2O).[38]

quantum yield of mono-protected **BP-PMB** and non-protected **BP** is significantly increased, which indicated that **βgal-BP-PMB** is a "turn on" type dual-responsive probe. **Mechanism of dual-responsive reactions**. Prior to examining the dual responsiveness, we investigated the mechanism of stepwise stimuli-responsive reactions of unsymmetric **BP** derivatives (Figure 3a). We recorded the UV-vis and PL spectra of **Ac-BP-PMB**, **BP-PMB**, and **BP**. As shown in Figures 3b and 3c (blue lines), **Ac-BP-PMB** has no obvious absorbance and emission in the UV-vis region. This is because two sterically demanding substituents at the oxygen functionality of **BP** cause a twisted structure. After the incubation of **Ac-BP-PMB** with pig liver esterase (PLE)[39–41] in pH 7.0 buffer solution at 40 °C for 24 h, the esterase-responsive Ac group of **Ac-BP-PMB PMB** was removed, affording moderately emissive **BP-PMB** (orange lines). Upon comparison with the UV-vis absorption and emission spectra of synthetically prepared **BP-PMB** (violet lines), we were able to confirm that the enzymatic reaction proceeded quantitatively, without

removal of the PMB group. It is known that the PMB protecting group is relatively stable under acidic conditions.[42] Surprisingly, after the adjustment of the pH value from 7.1 to 5.0, **BP-PMB** in the enzymatic reaction mixture smoothly converted to strongly emissive **BP** within 30 min (green lines). Furthermore, the PMB group could not be removed when **Ac-BP-PMB** was incubated in pH 5.0 buffer solution in the absence of PLE.
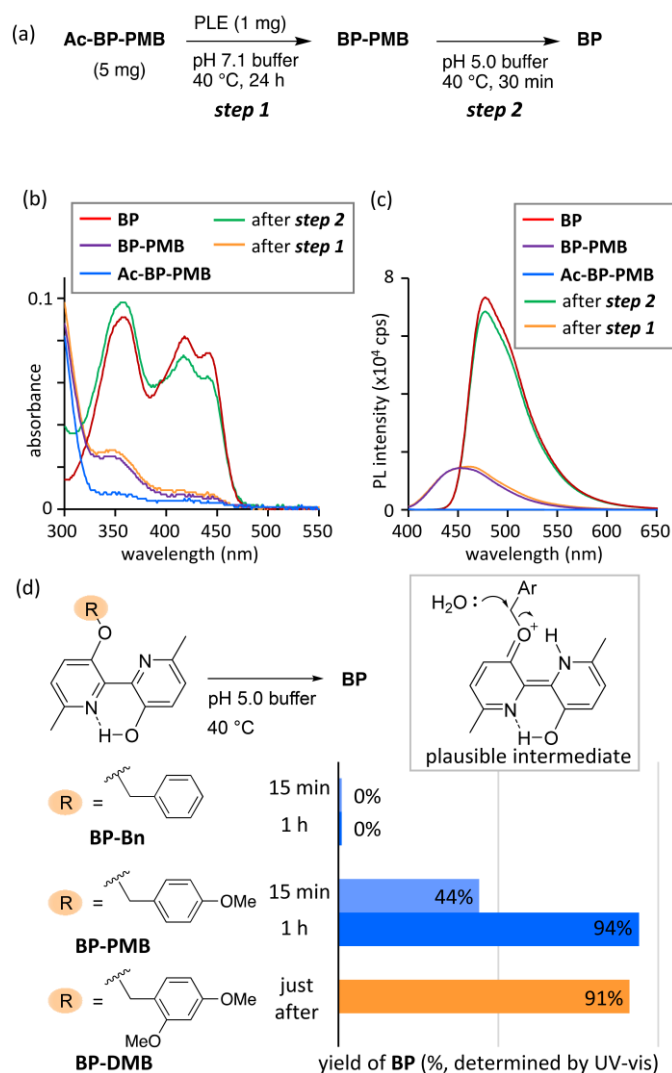

Figure 3. (a) Stepwise dual-responsive process of **Ac-BP-PMB**. (b) UV-vis absorbance and (c) photoluminescence spectra of **BP**, **BP-PMB**, and **Ac-BP-PMB** after the treatment of PLE for 24 h, and the enzymatic reaction mixture further incubated in pH 5.0 buffer for 30 min. λ_{ex}= 350 nm. Dye concentration = 10 µM. (d) Acid-responsiveness of **BP-Bn**, **BP-PMB**, and **BP-DMB** (10 µM).

To investigate further the mechanism of this phenomenon, we synthesized monosubstituted **BP-Bn** and **BP-DMB** by inducing a benzyl (Bn) group and a 2,4-dimethoxybenzyl (DMB) group (instead of the PMB group in **BP-PMB**), respectively. As expected, **BP-PMB** smoothly converted to **BP** in pH 5.0 buffer solution (Figure 3d). Although a Bn moiety remained intact under acidic conditions over a period of 1 h, 91% **BP-DMB** was immediately converted to **BP** in the pH 5.0 buffer solution. These results indicate that an electron-donating methoxy group contributes to the stabilization of the oxonium cation of **BP-PMB** formed under acidic conditions, which makes the nucleophilic attack by H_2O more likely to occur.[43] Having verified the dual responsiveness of the BP-based probe **Ac-BP-PMB**, we next focused our attention on the detection of β-gal to prove the versatility of the **BP** core.

Dual-responsiveness and selectivity of βgal-BP-PMB. To examine its enzyme responsiveness, we incubated **βgal-BP-PMB** (10 μM) with different concentrations of β-gal for 30 min (Figures 4a and 4b). The emission of the reaction mixture exhibited a good linear relationship in the β-gal concentration range 0–1 U/mL ($R^2 = 0.9937$). The limit of detection (LOD)[44] was determined to be 0.033 U/mL. These results indicate a high sensitivity of **βgal-BP-PMB** towards β-gal. When the PL of the reaction mixture of **βgal-BP-PMB** incubated with β-gal (10 μM) in pH 5.0 buffer was measured as a function of time (Figure 4c), significantly enhanced PL at 479 nm was observed after 30 min, indicating the high efficiency of **βgal-BP-PMB** in detecting the activity of β-gal under acidic conditions. The PL responses of **βgal-BP-PMB** towards a series of interfering species that may coexist with β-gal were determined. No PL signal was observed when **βgal-BP-PMB** was treated with an interfering species (see Figure S1).
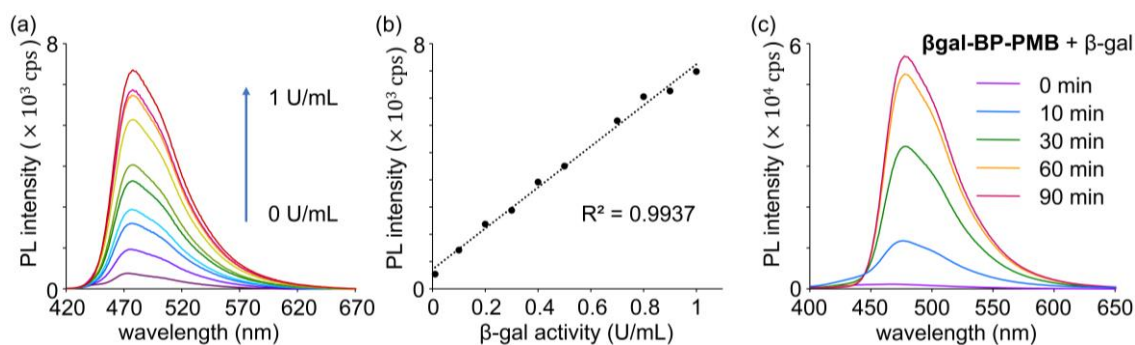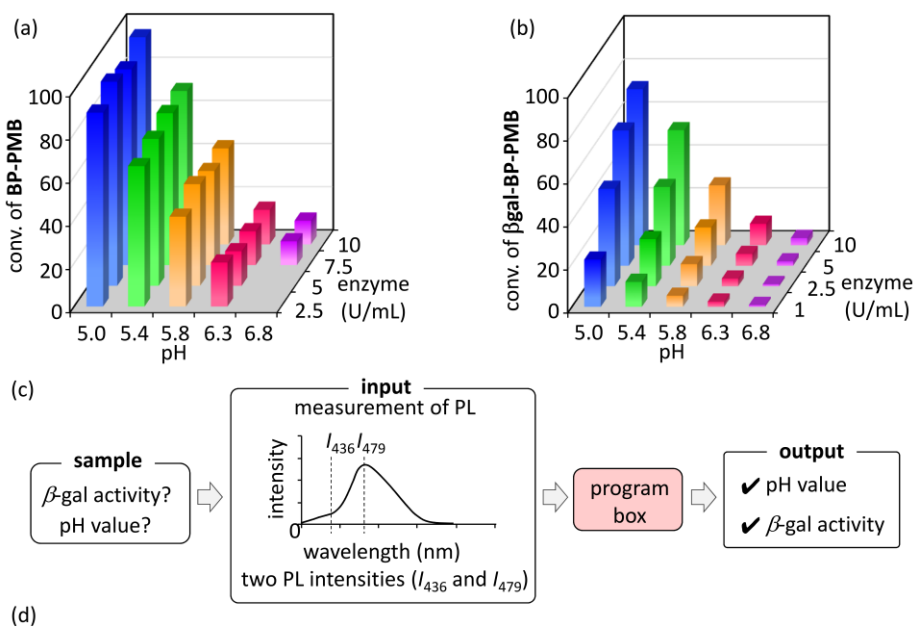
Figure 4. (a) Emission spectra and (b) linear plot of emission intensities at 479 nm when **βgal-BP-PMB** was treated with different concentration of β-gal at 37 °C for 10 min. (c) Photoluminescence spectra of the reaction mixture of **βgal-BP-PMB** (10 μM) with β-gal (10 U/mL) at 37 °C. Conditions: pH 5.0 buffer/DMF (v/v = 29/1), λ_{ex} = 350 nm.

	calc. pH (exp. pH)	relative error [p]	calc. EA (exp. EA) (U/mL)	relative error [q]
condition 1	5.77 (5.73)	0.70%	5.45 (6.00)	9.20%
condition 2	5.95 (5.98)	0.50%	7.44 (8.00)	7.00%
condition 3	5.57 (5.53)	0.72%	4.23 (4.00)	5.75%

Figure 5. Three-dimensions patterns of the conversion of (a) **BP-PMB** and (b) **βgal-BP-PMB**, with different pH and different β-gal activity. The conversion of **BP-PMB** and **βgal-BP-PMB** are defined as [**BP**] / ([**BP-PMB**] + [**BP**]) and ([**BP-PMB**] + [**BP**]) / [**βgal-BP-PMB**], respectively. (c) Flowchart program for determining pH value and enzyme activity of an unknown sample by ratiometric analysis. (d) Evaluation of the program

accuracy. Incubated with 10 μM **βgal-BP-PMB** at 37 °C for 30 min. The pH values (exp. pH) and β-gal activities (exp. EA) in prepared samples are shown in parentheses. Calculated pH values (calc. pH) and β-gal activities (calc. EA) were obtained by the program box shown in Figure 5c. [p] Relative error of pH value = |(calc. pH) – (exp. pH)| / (exp. pH). [q] Relative error of β-gal activity = |(calc. EA) – (exp. EA)| / (exp. EA).

Program for quantification of pH and β-gal activity. Taking advantage of the red-shifted emission band of **BP** compared with that of **BP-PMB** (Figure 3c), we next demonstrated the feasibility of monitoring both the pH and enzyme activity in an unknown sample by employing a chemometric technique. We first measured the emission spectra of a mixture of **BP-PMB** and **BP** (various ratios) (Figure S2). Based on the good linear relationships, the concentrations of **BP-PMB** and **BP** could be derived from PL at 436 nm and 479 nm, respectively. Three-dimensional patterns of the conversion of **βgal-BP-PMB** and **BP-PMB**, with different pH values and different β-gal activities, are shown in Figure 5. The conversion of **BP-PMB** was negatively correlated with the pH, but unaffected by β-gal activity (Figure 5a), indicating that the pH of an unknown sample can be estimated according to the conversion of **BP-PMB**. When the pH was held constant, the conversion of **βgal-BP-PMB** increased with increases in the β-gal activity (Figure 5b). Based on these unique correlations, we determined that **βgal-BP-PMB** can be applied to the measurement of pH and β-gal activity in an unknown sample.

We now propose the following calculation program (Figure 5c): (1) incubate **βgal-BP-PMB** with the unknown sample at 37 °C for 30 min, (2) measure the PL spectra of the reaction mixture and (3) input the PL intensity at 436 nm and 479 nm into the program box. The program box will automatically output the calculated pH and enzyme activity. This program can be easily established by other research groups. Only one further standard correction step is required to eliminate equipment error. As shown in Figure S4, after measuring the PL spectra of **BP** and **BP-PMB**, the coefficients a, b, c, and d can be adjusted. Further steps are illustrated in Figure S4.

To determine accuracy, we set up three conditions with different pH values and β-gal activities. As summarized in Figure 5d, relative errors in terms of the pH and β-gal activity

between their calculated and experimental values were 0.6% ± 0.1% and 7% ± 2%, respectively, hence demonstrating that this calculation program is highly reliable. To the best of our knowledge, this is the first ratiometric dual-responsive ratiometric probe enabling one to quantificationally monitor two analytes of interest in a sample to be assayed.

Living cell imaging. Inspired by the good β-gal responsiveness observed from *in vitro* measurements, we next attempted to evaluate its performance in living cells by incubating **βgal-BP-PMB** (10 μM) with the human ovarian cancer cell line OVK-18, which is known to exhibit high expression of endogenous β-gal (Figure 6a). Normal human umbilical vein endothelial cell line HUVEC and human cervix epithelial carcinoma cell line HeLa were incubated with **βgal-BP-PMB** (10 μM) as control groups. Confocal imaging revealed that PL was significantly enhanced in OVK-18 cells, as opposed to negligible signals in HUVEC and HeLa cells. Furthermore, **βgal-BP-PMB** showed almost no cytotoxicity, up to 10 μM, towards HeLa cells, HUVEC cells and OVK-18 in MTT assay (Figure S5). To confirm whether the enhanced PL was caused by the β-gal in OVK-18 cells, a control experiment was carried out using *D*-galactose as a competitive inhibitor of β-gal (Figure S6). A significantly decreased PL in OVK-18 cells was observed when the cells were pretreated with *D*-galactose (10 mg/mL) prior to incubation with **βgal-BP-PMB**. As NH_4Cl is known to increase the pH in lysosomes from 4.7 to 6.4,[45] a decrement in photoluminescent signal from NH_4Cl-pretreated OVK-18 cells was detected (Figure S6). Considering these results, we claim that **βgal-BP-PMB** can serve as a good probe for monitoring β-gal activity and detecting abnormal changes in the acidic conditions of lysosomes in OVK-18 cells.
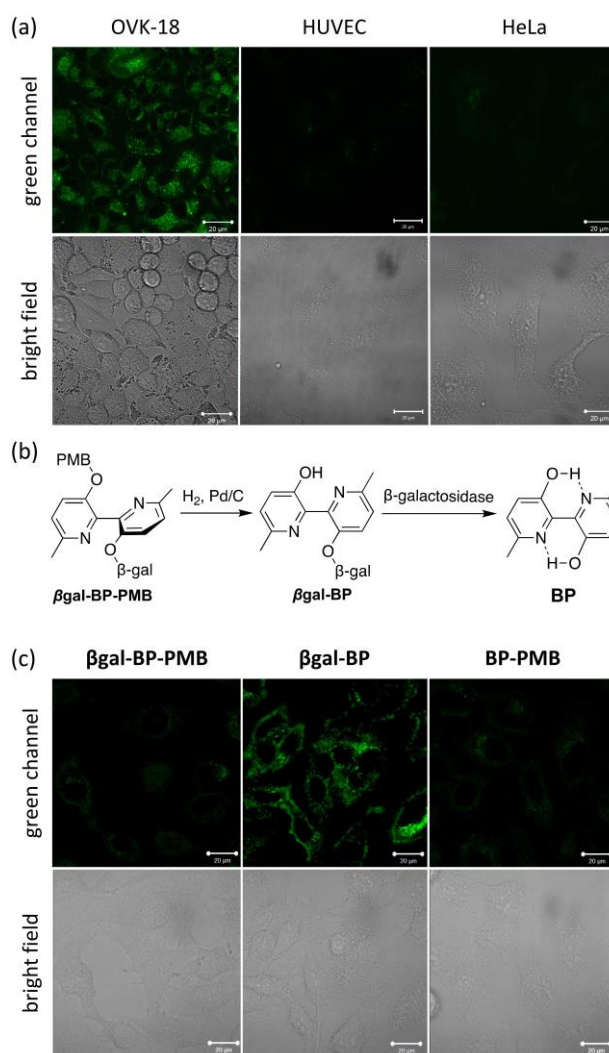
Figure 6. (a) Confocal images of HeLa, HUVEC, and OVK-18 after incubation with **βgal-BP-PMB** (10 μM) at 37 °C for 5 h. $\lambda_{ex}/\lambda_{det}$ = 405 nm/410–587 nm. Scale bar: 20 μm. (b) Synthesis and activation of **βgal-BP**. (c) Confocal images of HeLa cells. Cells pretreated with H_2O_2 (40 μM) for 2 h before incubation with **βgal-BP-PMB**, **βgal-BP**, and **BP-PMB**. $\lambda_{ex}/\lambda_{det}$ = 405 nm/410–587 nm. Scale: 20 μm.

To investigate whether this probe could distinguish ovarian cancer cells from senescent cells, further cell experiments were carried out. Probe **βgal-BP**, which has a β-gal-responsive group only, was synthesized through deprotecting PMB group (Figure 6b). The photophysical properties of **βgal-BP** were summarized in Table 1. It has been

reported that hydrogen peroxide (H_2O_2) can induce features of senescence in cells.[46] Three groups of HeLa cells were pretreated with H_2O_2 (40 μM) for 2 h to mimic senescent cells, and then treated separately with **βgal-BP-PMB**, **βgal-BP**, and **BP-PMB** (Figure 6c). Unpretreated HeLa cells were incubated with **βgal-BP** and **BP-PMB** (Figure S8) to confirm the β-gal expression level. As a result, the pH value in H_2O_2-induced senescent HeLa cells was increased and probe **βgal-BP** was activated in H_2O_2-pretreated cells, indicating that senescence-associated β-gal (SA-β-gal) activity was enhanced as expected. Conversely, the pH-responsive probe **BP-PMB** was silenced in H_2O_2-pretreated HeLa cells because of the increased pH value in lysosomes. The single-input activatable probe **βgal-BP** emitted strong signals in both senescent HeLa cells (Figure 6c) and OVK-18 cells (Figure S9). By contrast, **βgal-BP-PMB** emitted negligible photoluminescent signals in senescent HeLa cells (Figure 6c), but was selectively activated in OVK-18 cells (Figure 6a). Considering these results, it is evident that **βgal-BP-PMB** has the potential to detect ovarian cancer cells efficiently without the disturbance of false signals caused by senescent cells.

3. Conclusion

In conclusion, in this study, we designed and synthesized the first dual-responsive probes that enable the quantitative detection of two analytes with high reliability. To the best of our knowledge, this is the first report of a dual-responsive activatable ratiometric probe for the simultaneous quantification of both pH and enzyme activity, as well as one of the smallest photoluminescent cores useful for dual sensing. Furthermore, the acid- and β-gal-responsive probe **βgal-BP-PMB** could differentiate ovarian cancer cells from senescent cells that have similar β-gal overexpressed intracellular environments. Considering its simple design and versatile functionalization, we believe that the 3,3′-dihydroxy-2,2′-bipyridyl core could become one of the most powerful candidates in the probe library. Furthermore, it is expected that such dual-responsive small molecules will achieve their enormous potential in the area of bioimaging and offer new perspectives for a better understanding of complicated physiological processes.

4. Experimental

Marerials and reagents: Potassium carbonate (K_2CO_3) were purchased from Kishida Chemical Co., Ltd. (Japan). Acetic anhydride, tributyltin(IV) chloride (n-Bu_3SnCl), dichloromethane (CH_2Cl_2), hexane, copper(I) bromide, and acetonitrile (MeCN) were purchased from FUJIFILM Wako Pure Chemicals Co. (Japan). N,N-Dimethylformamide (DMF), methanol (MeOH), potassium fluoride (KF), Silver(I) oxide (Ag_2O), ethyl acetate (AcOEt), palladium on carbon (5% Pd/C), and tetrahydrofuran (THF) were purchased form nacalai tesque (Japan). Celite®535 was purchased from Signa-Aldrich (United States). n-Butyl lithium (n-BuLi, in hexane, 1.6 M) were purchased from Tokyo Chemical Industry (TCI) Co., Ltd. (Japan). Silica gel (SiO_2, 230–400 mesh) for column chromatography was purchased from Silicycle (Canada). Buffered aqueous solutions (pH 1.2) were prepared by dissolving hydrochloric acid (HCl) and potassium chloride (KCl) in water (MilliQ). Buffered aqueous solutions (pH 2.6–6.3) were prepared by dissolving citric acid and sodium dihydrogenphosphate (NaH_2PO_4) in water (MilliQ). Buffered aqueous solutions (pH 6.8–8.0) were prepared by dissolving NaH_2PO_4 and disodium hydrogenphosphate (Na_2HPO_4) in water (MilliQ). All buffered aqueous solutions were stored in refrigerator and used within one week. Solvents were distillated under N_2 atmosphere by using CaH_2 or Mg as drying agents before use.

Instruments: UV-Vis absorption spectra were measured by UV-vis-NIR spectrophotometer (UH5300, Hitachi High-Technologies Co., Japan). Emission spectra were measured by fluorescence spectrophotometer (RF-6000, Shimadzu Co., Japan). High resolution mass spectra were measured by EXACTIVE (ESI, Thermo Fisher Scientific Inc., USA). NMR spectra were recorded on JEOL ECZ-400 spectrometer.

Compound 1: Under nitrogen atmosphere, to a solution of 2-iodo-3-[(4-methoxyphenyl)methoxy]-6-methylpyridine (**P1a** in SI, 3.4 g, 9.5 mmol) in THF (80 mL) was added n-BuLi (7.4 mg, 12 mmol, 1.6 M in hexane) at –78 °C, and the resulting mixture was stirred at –78 °C for 15 min. To this solution was added n-Bu_3SnCl (3.9 mL, 14 mmol) at –78 °C and the resulting mixture was stirred at room temperature for 19 h. Saturated KF aqueous solution was added to the reaction mixture and the resulting mixture was stirred for 30 min, then filtered through a Celite pad. The filtrate was concentrated under vacuum to remove THF and the residue was dissolved in AcOEt (20 mL). The organic layer was washed with brine (2 × 30 mL) and saturated KF aqueous

solution (2 × 30 mL) and dried over anhydrous Na_2SO_4. After removal of solvent, the residue was purified by silica gel column chromatography (hexane/AcOEt, v/v = 20:1–7:1) to give **1** (3.9 g, 7.5 mmol, 79%) as a pale-yellow oil. IR (ATR) 1070, 1247, 1429, 1516, 2955 cm^{-1}; ^{1}H NMR (400 MHz, CDCl$_3$, 25 °C): δ = 0.87 (t, J = 7.3 Hz, 9H), 0.97–1.15 (m, 6H), 1.20–1.38 (m, 6H), 1.41–1.61 (m, 6H), 2.51 (s, 3H), 3.83 (s, 3H), 4.91 (s, 2H), 6.83–6.91 (m, 4H), 7.33 (d, J = 8.7 Hz, 2H). ^{13}C NMR (100 MHz, CDCl$_3$, 25 °C): δ = 10.0, 13.7, 23.7, 27.3, 29.0, 55.2, 69.8, 113.8, 115.2, 121.2, 128.7, 129.4, 151.1, 157.9, 159.4, 163.3. HRMS (ESI) calcd for $C_{27}H_{42}NO_{43}Sn$ ([M+H]$^+$): 520.2238, found: 520.2243.

Compound 2: 3-Hydroxy-2-iodo-6-methylpyridine (5.9 g, 17 mmol) was dissolved in acetic anhydride (8.8 mL) and the mixture was stirred at 110 °C for 3.5 h. After diluted by AcOEt (20 mL), the mixture was washed by saturated NaHCO$_3$ (2 × 30 mL). The organic layer was dried over anhydrous Na$_2$SO$_4$. After removal of solvent, the residue was purified by recrystallization to give **2** (3.9 g, 14 mmol, 83%) as a yellowish-brown solid. mp: 62.4–63.8 °C; IR (ATR) 645, 828, 858, 897, 1009, 1056, 1183, 1243, 1348, 1368, 1439,1559, 1767 cm^{-1}; ^{1}H NMR (400 MHz, CDCl$_3$, 25 °C): δ = 2.38 (s, 3H), 2.46 (s, 3H), 7.11 (d, J = 7.6 Hz, 1H), 7.23 (d, J = 7.6 Hz, 1H). ^{13}C NMR (100 MHz, CDCl$_3$, 25 °C): δ = 21.2, 23.6, 114.2, 123.1, 130.0, 146.4, 157.8, 168.4. HRMS (ESI) calcd for $C_8H_8INO_2$ ([M+H]$^+$): 277.9678, found: 277.9678

Ac-BP-PMB: Under nitrogen atmosphere, **1** (3.5 g, 6.8 mmol), **2** (1.9 g, 6.8 mmol), Pd(PPh$_3$)$_4$[47] (0.39 g, 5.0 mol%), and CuBr (68 mg, 7.0 mol%) were added to DMF (80 mL) and the resulting mixture was stirred at 110 °C for 19 h. Saturated KF aqueous solution was added to the reaction mixture and the resulting mixture was stirred for 30 min, then filtered through a Celite pad. The filtrate was diluted by AcOEt (20 mL). The organic layer was washed with brine (2 × 30 mL) and saturated KF aqueous solution (2 × 30 mL) and dried over anhydrous Na$_2$SO$_4$. After removal of solvent, the residue was purified by silica gel column chromatography (hexane/AcOEt, v/v = 1:1 to AcOEt only) to give **Ac-BP-PMB** (1.6 g, 4.2 mmol, 62%) as an orange oil. IR (ATR) 826, 1033, 1200, 1249, 1369, 1446, 1515, 1767 cm^{-1}; ^{1}H NMR (400 MHz, CDCl$_3$, 25 °C): δ = 2.06 (s, 3H), 2.54 (s, 3H), 2.62 (s, 3H), 3.77 (s, 3H), 4.91 (s, 2H), 6.79 (d, J = 8.7 Hz, 2H), 7.08 (d, J = 8.7 Hz, 1H), 7.13 (d, J = 8.2 Hz, 2H), 7.17-7.22 (m, 2H), 7.49 (d, J = 8.2 Hz, 1H). ^{13}C

NMR (100 MHz, CDCl$_3$, 25 °C): δ = 20.9, 23.6, 24.1, 55.2, 71.4, 113.7, 122.6, 123.3, 123.7, 128.4, 128.8, 130.9, 143.6, 145.4, 147.8, 150.9, 151.1, 155.7, 159.2, 168.6. HRMS (ESI) calcd for C$_{22}$H$_{22}$N$_2$O$_4$ ([M+H]$^+$): 569.1622, found: 569.1631.

BP-PMB: To an aqueous solution of K$_2$CO$_3$ (64 mg, 0.46 mmol) was added a MeOH solution of **Ac-BP-PMB** (0.16 g, 0.42 mmol) and the resulting mixture was stirred at room temperature for 4 h. Then the mixture was concentrated under vacuum to remove MeOH and the residue was dissolved in AcOEt (20 mL). The organic layer was washed with brine (30 mL × 3) and dried over anhydrous Na$_2$SO$_4$. After removal of solvent, the residue was purified by silica gel column chromatography (hexane/AcOEt, v/v = 10:1–2:1) to give 0.15 g (quant) of yellow solid **BP-PMB**. mp: 78.5–79.5 °C; IR (ATR) 652, 744, 823, 1033, 1058, 1143, 1175, 1246, 1278, 1456, 1514, 1573, 1614, 2922 cm^{-1}; ^{1}H NMR (400 MHz, CDCl$_3$, 25 °C): δ = 2.52 (s, 3H), 2.55 (s, 3H), 3.82 (s, 3H), 5.13 (s, 2H), 6.90 (d, J = 8.7 Hz, 2H), 7.06 (d, J = 8.2 Hz, 1H), 7.13 (d, J = 8.7 Hz, 1H), 7.22 (d, J = 8.7 Hz, 1H), 7.41 (d, J = 8.2 Hz, 1H), 7.49 (d, J = 8.7 Hz, 2H). ^{13}C NMR (100 MHz, CDCl$_3$, 25 °C): δ = 22.8, 23.7, 55.2, 71.8, 113.6, 123.3, 124.6, 125.5, 126.1, 128.7, 128.9, 137.2, 146.6, 147.0, 147.4, 151.6, 153.7, 159.2. HRMS (ESI) calcd for C$_{20}$H$_{21}$N$_2$O$_3$ ([M+H]$^+$): 337.1552, found: 337.1555.

βgal-BP-PMB: Under nitrogen atmosphere, a solution of **BP-PMB** (0.3 g, 0.89 mmol), 2,3,4,6-tetra-O-acetyl-alpha-D-galactopyranosyl bromide[48] (0.4 g, 1.8 mmol), and Ag$_2$O (0.7 g, 1.9 mmol) in MeCN (20 mL) was stirred at 60 °C for 12 h. The reaction mixture was cool down to room temperture and filtered through a Celite pad. The filtrate was concentrated under vacuum to remove MeCN. The residue and Na$_2$CO$_3$ (1.8 g, 16.8 mmol) were added to a solution of MeOH/MeCN/H$_2$O (v/v/v = 4/4/3, 50 mL) and the resulting solution was stirred at room temperature for 2 h. Then the mixture was concentrated under vacuum to remove MeOH and MeCN. After neutralized with 10% HCl, the whole was extracted with AcOEt (20 mL). The organic layer was washed with brine (30 mL × 3) and dried over anhydrous Na$_2$SO$_4$. After removal of solvent, the residue was purified by silica gel column chromatography (CH$_2$Cl$_2$/MeOH, v/v = 20:1–5:1) to give **βgal-BP-PMB** (0.17 g, 0.34 mmol, 38.2%) as a yellow solid. mp: 105.3–107.0 °C; IR (ATR) 509, 522, 822, 1071, 1252, 1451, 1515 cm^{-1}; ^{1}H NMR (400 MHz, CDCl$_3$, 25 °C): δ = 2.51 (s, 3H), 2.56 (s, 3H), 3.63–3.67 (m, 2H), 3.74–3.76 (m, 1H), 3.77 (s, 3H),

3.86–3.90 (m, 1H), 3.98–4.03 (m, 2H), 4.77 (d, J = 7.8 Hz, 1H), 4.89 (d, J = 12 Hz, 1H), 4.99 (d, J = 12 Hz, 1H), 6.80 (d, J = 8.7 Hz, 2H), 7.11–7.17 (m, 4H), 7.30 (d, J = 8.7 Hz, 1H), 7.57 (d, J = 8.2 Hz, 1H). ^{13}C NMR (100 MHz, CDCl$_3$, 25 °C): δ = 22.8, 23.6, 55.2, 61.6, 68.5, 70.6, 71.5, 73.0, 75.1, 104.5, 113.8, 124.0, 124.1, 126.2, 128.3, 128.9, 145.7, 145.9, 149.7, 150.0, 151.5, 152.2, 159.3, 162.7. HRMS (ESI) calcd for C$_{26}$H$_{31}$N$_2$O$_8$ ([M+H]$^+$): 499.2080, found: 499.2086.

βgal-BP: A mixture of **βgal-BP-PMB** (30 mg, 0.06 mmol), 5% Pd/C (4 mg) and dry MeOH (1 mL) was stirred under hydrogen atmosphere (balloon) at rt for 3 h. The reaction mixture was filtered through a Celite pad. The filtrate was concentrated under vacuum to remove MeOH. After removal of solvent, the residue was pure enough to give 23 mg (quant) as a white solid **βgal-BP**. IR (ATR) 656, 697, 757, 823, 881, 1021, 1061, 1092, 1137, 1283, 1488, 1575 cm^{-1}; ^{1}H NMR (400 MHz, d$_6$-DMSO, 25 °C): δ = 2.69 (s, 3H), 2.56 (s, 3H), 3.19 (d, J = 6.8 Hz, 1H), 4.57 (t, J = 5.1 Hz, 1H), 4.75 (d, J = 6.6 Hz, 1H), 4.79 (d, J = 9.8 Hz, 1H), 4.94 (t, J = 7.4 Hz, 1H), 7.20 (d, J = 10.8 Hz, 1H), 7.29 (d, J = 10.3 Hz, 1H), 7.37 (d, J = 10.3 Hz, 1H), 7.74 (d, J = 10.8 Hz, 1H). ^{13}C NMR (100 MHz, d$_6$-DMSO, 25 °C): δ = 22.8, 23.0, 60.7, 68.3, 70.7, 72.6, 76.3, 104.9, 124.4, 124.9, 125.8, 127.2, 139.9, 145.1, 147.5, 150.0, 150.6, 151.7. HRMS (ESI) calcd for C$_{18}$H$_{22}$N$_2$O$_7$Na ([M+Na]$^+$): 401.1319, found: 401.1326.

References

1. H. Singh, K. Tiwari, R. Tiwari, S. K. Pramanik, A. Das, *Chem. Rev.* **2019**, *119*, 11718–11760.
2. X. Li, X. Gao, W. Shi, H. Ma, *Chem. Rev.* **2014**, *114*, 590–659.
3. J. Chan, S. C. Dodani, C. J. Chang, *Nat. Chem.* **2012**, *4*, 973–984.
4. H. Zhu, J. Fan, J. Du, X. Peng, *Acc. Chem. Res.* **2016**, *49,* 2115–2126.

5. J. Li, F. Cheng, H. Huang, L. Li, J. J. Zhu, *Chem. Soc. Rev*. **2015**, *44*, 7855–7880.

6. H. Kobayashi, P. L. Choyke, *Acc. Chem. Res*. **2011**, *44*, 83–90.

7. J. F. Lovell, T. W. B. Liu, J. Chen, G. Zheng, *Chem. Rev*. **2010**, *110*, 2839–2857.

8. J. Zhang, P. Cheng, K. Pu, *Bioconjugate Chem*. **2019**, *30*, 2089–2101.

9. Y. Zhang, C. Yan, C. Wang, Z. Guo, X. Liu, W. H. Zhu, *Angew. Chem. Int. Ed*. **2020**, *59*, 9059–9066.

10. J. A.Chen, H. Pan, Z. Wang, J. Gao, J. Tan, Z. Ouyang, W. Guo, X. Gu, *Chem. Commun*. **2020**, *56*, 2731–2734.

11. J. N. Makau, A. Kitagawa, K. Kitamura, T. Yamaguchi, S. Mizuta, *ACS Omega* **2020**, *5*, 11299–11307.

12. X. Li, Y. Pan, H. Chen, Y. Duan, S. Zhou, W. Wu, S. Wang, B. Liu, *Anal. Chem*. **2020**, *92*, 5772–5779.

13. Y.Li, L. Ning, F. Yuan, T. Zhang, J. Zhang, Z. Xu, X. F. Yang, *Anal. Chem*. **2020**, *92*, 5733–5740.

14. G. P. Dimri, X. Lee, G. Basile, M. Acosta, G. Scott, C. Roskelley, E. E. Medrano, M. Linskens, I. Rubelj, O. A. Pereira-Smith, M.Peacocke, J. Campisi, *Proc. Natl Acad. Sci. USA* **1995**, *92*, 9363–9367.

15. B. Y. Lee, J. A. Han, J. S. Im, A. Morrone, K. Johung, E. C. Goodwin, W. J. Kleijer, D. DiMaio, E. S. Hwang, *Aging Cell* **2006**, *5*, 187–195.

16. J. L. Kolanowski, F. Liu, E. J. New, *Chem. Soc. Rev.* **2018**, *47*, 195–208.

17. B.Finkler, I. Riemann, M. Vester, A. Grüter, F. Stracke, G. Jung, *Photochem. Photobiol. Sci.* **2016**, *15*, 1544–1557.

18. J. B. Grimm, T. D. Gruber, G. Ortiz, T. A. Brown, L. D. Lavis, *Bioconjugate Chem*. **2016**, *27*, 474–480.

19. S.Debieu, A. Romieu, *Org. Biomol. Chem*. **2015**, *13*, 10348–10361.

20. M. Prost, J. Hasserodt, *Chem. Commun*. **2014**, *50*, 14896–14899.

21. Y. Fang, W. Shi, Y. Hu, X. Li, H. Ma, *Chem. Commun*. **2018**, *54*, 5454–5457.

22. S. Y. Li, L. H. Liu, H. Cheng, B. Li, W. X. Qiu, X. Z. Zhang, *Chem. Commun*. **2015**, *51*, 14520–14523.

23. Y. Li, H. Wang, J. Li, J. Zheng, X. Xu, R. Yang, *Anal. Chem.* **2011**, *83,* 1268–1274.

24. S. H. Park, N. Kwon, J. H. Lee, J. Yoon, I. Shin, *Chem. Soc. Rev*. **2020**, *49*, 143–179.

25. G. Bunt, F. S. Wouters, *Biophys. Rev.* **2017**, *9,* 119–129.

26. R. Zhang, F. Yan, Y. Huang, D. Kong, Q. Ye, J. Xu, L. Chen, *Adv.* **2016**, *6*, 50732–50760.

27. L. Yuan, W. Lin, K. Zheng, S. Zhu, *Acc. Chem. Res.* **2013**, *46*, 1462–1473.

28. K. E. Sapsford, L. Berti, I. L. Medintz, *Angew. Chem. Int. Ed.* **2006**, *45*, 4562–4588.

29. R. Dutta, A. Pyne, D. Mondal, N. Sarkar, *ACS Omega* **2018**, *3*, 314–328.

30. O. K. Abou-Zied, *J. Phys. Chem. B* **2010**, *114*, 1069–1079.

31. F. Plasser, M. Barbatti, A. J. A. Aquino, H. Lischka, *J. Phys. Chem. A* **2009**, *113*, 8490–8499.

32. L. He, B. Dong, Y. Liu, W. Lin, *Chem. Soc. Rev.* **2016**, *45*, 6449–6461.

33. A. Romieu, *Org. Biomol. Chem.* **2015**, *13*, 1294–1306.

34. A. C. Sedgwick, L. Wu, H. H. Han, S. D. Bull, X. P. He, T. D. James, J. L. Sessler, B. Z. Tang, H. Tian, J. Yoon, *Chem. Soc. Rev.* **2018**, *47*, 8842–8880.

35. P. Zhou, K. Han, *Acc. Chem. Res.* **2018**, *51*, 1681–1690.

36. C. Naumann, H. Langhals, *Synthesis* **1990**, 279–281.

37. Y. Singh, A. V. Demchenko, *Chem. Eur. J.* **2019**, *25*, 1461–1465.

38. T. Härd, P. Fan, D. R. Kearns, *Photochem. Photobiol.* **1990**, *51*, 77-86.

39. K. M. Dillon, R. J. Carrazzone, Y. Wang, C. R. Powell, J. B. Matson, *ACS Macro Lett.* **2020**, *9*, 606–612.

40. K. Okada, T. Yamaguchi, K. Dodo, M. Sodeoka, S. Obika, *Bioorg. Med. Chem.* **2019**, *27*, 1444–1448.

41. K. K. Abney, S. J. Ramos-Hunter, I. M. Romaine, J. S. Goodwin, G. A. Sulikowski, C. D. Weaver, *Chem. Eur. J.* **2018**, *24*, 8985–8988.

42. P. G. M. Wuts, *Greene's Protecting Groups in Organic Synthesis*, 5th ed.; John Wiley & Sons: Hoboken, NJ, 2014.

43. E. O. Nwoye, G. B. Dudley, *Chem. Commun.* **2007**, *14*, 1436–1437.

44. W. Wang, K. Vellaisamy, G. Li, C. Wu, C. N. Ko, C. H. Leung, D. L. Ma, *Anal. Chem.* **2017**, *89*, 11679–11684.

45. S. Ohkuma, B. Poole, *Proc. Natl. Acad. Sci. USA.* **1978**, *75*, 3327–3331.

46. C. Bladier, E. J. Wolvetang, P. Hutchinson, J. B. de Haan, I. Kola, *Cell Growth Differ.* **1997**, *8*, 589–598.

47. D. R. Coulson, L. C. Satek, S. O. Grim, *Inorganic Syntheses, Vol. 13* (Eds.: F. A. Cotton), McGraw-Hill, NYC., **1972**, pp. 121.

48. S. E. Tasai, J. C. Lee, N. Uramaru, H. Takayama, G. J. Huang, F. F. Wong, *Heteroatom Chem.* **2017**, *28*, 21372.